Research Square

Preprints are preliminary reports that have not undergone peer review.
They should not be considered conclusive, used to inform clinical practice,
or referenced by the media as validated information.

Hybrid Quantum-Behaved and Bio-Swarm Optimization Algorithm (BioQPSO)

Manav Manav

manav-ug23@nsut.ac.in

Netaji Subhas University of Technology

Research Article

Keywords: Quantum-behaved particle swarm optimization, Bio-swarm intelligence, Hybrid metaheuristic, Ant colony optimization, Artificial bee colony, Benchmark optimization, Feature selection, Swarm intelligence, Convergence analysis, Exploration–exploitation balance

Posted Date: March 25th, 2026

DOI: https://doi.org/10.21203/rs.3.rs-9178752/v1

License: This work is licensed under a Creative Commons Attribution 4.0 International License.
Read Full License

Additional Declarations: No competing interests reported.

Hybrid Quantum-Behaved and Bio-Swarm Optimization Algorithm (BioQPSO)

Manav[1]

Department of Electronics and Communication,
Netaji Subhas University of Technology, Delhi, India
manav-ug23@nsut.ac.in

Abstract. Quantum-Behaved Particle Swarm Optimization (QPSO) offers strong global search ability but can suffer from reduced adaptability on certain multimodal and biologically structured search landscapes. This paper proposes BioQPSO, a hybrid framework that integrates QPSO's quantum-probabilistic position update model with bio-inspired swarm intelligence mechanisms drawn from ant colony and bee foraging behavior. Two concrete variants are introduced: AntBioQPSO, which incorporates pheromone-guided local leader selection and neighborhood communication, and BeeBioQPSO, which employs fitness-based local leadership and scout-driven reinitialization to counter stagnation. Both variants extend the standard QPSO attractor by a third bio-inspired component with weight ϕ_3, yielding a three-term weighted attractor that balances personal, global, and neighborhood guidance. The proposed algorithms are evaluated on ten standard benchmark functions (unimodal and multimodal, $D = 30$) over 30 independent runs with 30 particles and 1000 iterations, and compared against PSO, QPSO, Ant Colony Optimization (ACO), and Artificial Bee Colony (ABC). Statistical validation using Wilcoxon signed-rank and Friedman tests confirms significant performance differences across all benchmarks ($p < 10^{-9}$ in all cases). In a real-world feature selection task on the Wisconsin Breast Cancer dataset (569 samples, 30 features), BeeBioQPSO achieves 94.83% classification accuracy using only 2 features on average, with the lowest standard deviation (0.49%) among all tested algorithms. These results demonstrate that the BioQPSO framework provides a competitive and robust platform for complex optimization, with particular strengths on multimodal functions and practical feature selection tasks.

Keywords: Quantum-behaved particle swarm optimization · Bio-swarm intelligence · Hybrid metaheuristic · Ant colony optimization · Artificial bee colony · Benchmark optimization · Feature selection · Swarm intelligence · Convergence analysis · Exploration–exploitation balance

1 Introduction

Quantum-inspired optimization techniques are emerging as effective methods for tackling complex problems. Methods like Hybrid Quantum-Inspired Swarm

Optimization (HQISO) and hybrid clustering algorithms combining quantum-behaved particle swarm optimization and K-harmonic means (HQPSO) show promise when compared to established algorithms such as Particle Swarm Optimization (PSO) and Genetic Algorithm (GA), demonstrating enhanced performance in various optimization tasks [14,12]. PSO simulates the social interaction of particles moving through a multidimensional search space, dynamically adjusting their trajectories toward the best-known personal and global positions. Despite its popularity, classical PSO suffers from premature convergence and limited diversity when tackling multimodal functions.

To overcome these limitations, Quantum-Behaved Particle Swarm Optimization (QPSO) was introduced by Sun et al. [15], incorporating principles from quantum mechanics to redefine particle motion through probability density functions rather than explicit velocities. By modeling particles as quantum entities distributed within potential wells, QPSO has fewer parameters and high capability in solving challenging optimization problems while remaining simple to implement. Since then, many studies have extended QPSO with respect to traditional machine learning methods.

However, while QPSO achieves superior convergence behavior compared to classical PSO, it can still experience reduced adaptability when addressing dynamically changing or biologically inspired search domains. To enhance adaptability and resilience, recent research has explored bio-inspired swarm algorithms such as the Artificial Bee Colony (ABC) [10], Firefly Algorithm (FA) [16], and Bacterial Foraging Optimization (BFO) [5], which emulate natural behaviors like cooperation, adaptation, and reproduction for distributed problem solving. These algorithms exhibit strong local refinement and dynamic population adaptation but often lack QPSO's global probabilistic balance.

In this context, this paper proposes the Hybrid Quantum-Behaved and Bio-Swarm Optimization Algorithm (BioQPSO)—a framework that integrates QPSO's quantum search model with the adaptive behavioral characteristics of bio-swarm intelligence. The core novelty of BioQPSO, distinguishing it from existing hybrid PSO/QPSO works, is its *three-term attractor formulation*: the standard two-term QPSO attractor (personal best + global best) is extended by an explicit bio-inspired neighborhood guidance term weighted by ϕ_3. Most existing hybrids append bio-swarm operators as external perturbation or diversity-restoration steps applied *after* the base PSO/QPSO update; BioQPSO instead embeds the bio signal *directly* into the quantum attractor, so that every position update already reflects local neighborhood intelligence. This architectural difference means that exploration–exploitation balance is governed at the fundamental update level rather than through separate, potentially competing mechanisms. Two instantiations are proposed—AntBioQPSO (pheromone-guided local leadership) and BeeBioQPSO (fitness-based leadership with scout reinitialization)— and both are compared head-to-head against the pure ACO and ABC algorithms that inspired them, a comparison absent from prior hybrid QPSO literature.

The original PSO algorithm, while widely used, suffers from several inherent limitations: susceptibility to premature convergence, slow convergence dur-

ing fine-tuning phases, and weak exploratory capabilities on highly multimodal landscapes [11]. These limitations have motivated the development of advanced variants and hybrid algorithms that improve global search ability, convergence rate, and robustness across varied problem domains.

The remainder of this paper is organized as follows. Section 2 reviews related work on swarm intelligence and hybrid QPSO approaches. Section 3 describes the methodology, covering PSO, bio-swarm intelligence, QPSO, and the proposed BioQPSO framework in detail. Section 4 presents experimental results on ten benchmark functions and a real-world feature selection task, together with statistical analysis. Section 5 presents a sensitivity analysis of the key BioQPSO parameters. Section 6 concludes the paper and outlines directions for future work.

2 Related Work

Research in swarm intelligence has produced numerous advances for complex optimization, with PSO among the most prominent techniques. Classical PSO is frequently hindered by premature convergence and local optima entrapment, especially in high-dimensional or multimodal landscapes, motivating a broad family of hybrid and adaptive variants.

Yao et al. [17] introduced Hybrid Strategy PSO (HSPSO), integrating adaptive weight adjustment, reverse learning, Cauchy mutation, and the Hook–Jeeves strategy to enhance both exploration and exploitation. Empirical evaluations on CEC-2005 and CEC-2014 suites demonstrate superiority over traditional PSO, DAIW-PSO, HBF-PSO, BOA, ACO, and FA. The authors further validate HSPSO on feature selection for the UCI Arrhythmia dataset, achieving high classification accuracy—reaffirming the value of hybrid adaptive strategies for real-world machine learning tasks.

QPSO [15] enhances classical PSO by modeling particles as quantum entities moving under probability density functions, eliminating the velocity vector and reducing the parameter count. Hybrid QPSO variants have demonstrated improved search diversity and robustness [8,18]. Recent work has further coupled QPSO with deep learning [14] and adaptive neighborhood topologies [12], extending its applicability to dynamic and large-scale problems.

On the bio-inspired side, the Artificial Bee Colony (ABC) [10] partitions agents into employed, onlooker, and scout roles to balance local exploitation and global exploration. Ant Colony Optimization (ACO), originally developed for combinatorial problems [5], has been adapted to continuous domains through Gaussian kernel-based sampling (ACO_R), offering competitive performance on standard benchmarks. Recent surveys on hybrid swarm methods highlight that combining multiple behavioral paradigms can yield algorithms that are more robust than any single constituent [16,11].

Metaheuristic algorithms have also proven highly effective in real-world machine learning tasks such as intrusion detection and feature selection. Alzubi et al. [2] proposed an SVM-based malware detector whose hyperparameters and

feature weights are jointly optimized by Harris Hawks Optimization, achieving state-of-the-art detection rates on Android malware datasets. In a follow-up line of work, the same group coupled a Quantum Mayfly Optimization algorithm with an encoder-decoder LSTM network for malware classification [3], and applied a Salp Swarm Algorithm to optimize a multilayer perceptron for IoT intrusion detection, reporting accuracy above 97% on three independent benchmarks [4]. These works underscore the practical utility of hybridizing quantum-inspired search with bio-swarm mechanisms for classification and feature selection tasks. Movassagh et al. [13] further demonstrated that integrating invasive weed optimization with differential evolution for ANN training produces consistently better convergence than stand-alone metaheuristics, reinforcing the case for multi-paradigm hybridization. Most recently, Alzubi et al. [1] extended this line of inquiry to feature-weighted classification, demonstrating that swarm-driven feature selection significantly reduces model complexity without sacrificing accuracy.

Taken together, these works establish two recurring themes: (i) bio-swarm mechanisms are highly effective at feature selection and weight optimization for classifiers; and (ii) quantum-inspired search provides strong global exploration that complements local bio-swarm guidance. Prior hybrid approaches, however, typically combine only two behavioral sources—e.g., quantum + one bio-paradigm—and embed the bio-component as a post-processing or parameter-scheduling module rather than directly within the quantum attractor. This limits their ability to exploit topological neighborhood information during the core position update.

The present work addresses this gap by (i) hybridizing QPSO with *both* ant and bee mechanisms simultaneously via a unified three-term attractor; (ii) comparing the resulting hybrids directly against the pure bio-swarm algorithms (ACO and ABC) that inspired them; and (iii) validating on a real-world feature selection task. To the best of our knowledge, no prior work has addressed all three simultaneously.

3 Methodology

3.1 Experimental Assumptions

Unless stated otherwise, all simulations in this paper adopt the following assumptions: (i) all benchmark problems are minimization tasks in $D = 30$ dimensions; (ii) particle positions are initialized uniformly at random within the specified search bounds; (iii) each algorithm is run for 30 independent trials with 30 particles and 1000 iterations; (iv) the contraction-expansion coefficient β in QPSO-based variants is linearly decreased from 1.0 to 0.5 over the run; (v) all algorithms share identical random seeds across comparable runs to ensure fair statistical comparison; and (vi) no external datasets were used—all data were generated through simulation.

3.2 Particle Swarm Optimization (PSO)

Particle Swarm Optimization (PSO) is a well-known swarm intelligence-based optimization technique originally proposed by Kennedy and Eberhart in 1995 [7]. The method was inspired by the social behavior of bird flocking and fish schooling. At each iteration, the velocity $v_i(t)$ and position $x_i(t)$ of each particle i are updated as:

$$v_i(t+1) = w\, v_i(t) + c_1 r_1 \big(p_i^{\text{best}} - x_i(t)\big) + c_2 r_2 \big(g^{\text{best}} - x_i(t)\big) \quad (1)$$

$$x_i(t+1) = x_i(t) + v_i(t+1) \quad (2)$$

where p_i^{best} is the personal best position of particle i; g^{best} is the global best position found by the swarm; w is the inertia weight; c_1 and c_2 are the cognitive and social learning factors; and $r_1, r_2 \sim U(0,1)$ are uniform random variables. In our experiments we use $w = 0.729$, $c_1 = c_2 = 1.494$, following standard recommendations.

The pseudo-code of the PSO algorithm is illustrated in Algorithm 1.

Algorithm 1 PSO Algorithm

Input: population size M; bounds $[lb, ub]$; dimension D; coefficients c_1, c_2; maximum iterations *MaxIt*
Output: solution with best fitness value
Initialize positions X and velocities V uniformly at random
Evaluate fitness; set p_{best} and g_{best}
for $t = 1$ to *MaxIt* **do**
  for $i = 1$ to M **do**
    Sample $r_1, r_2 \sim U(0,1)$ and set $w \in [0,1]$
    for $j = 1$ to D **do**
      $V_{i,j}(t+1) \leftarrow wV_{i,j}(t) + c_1 r_1 (p_{\text{best}_{i,j}} - X_{i,j}(t)) + c_2 r_2 (g_{\text{best}_j} - X_{i,j}(t))$
      $X_{i,j}(t+1) \leftarrow \text{clip}\big(X_{i,j}(t) + V_{i,j}(t+1),\ lb,\ ub\big)$
    end for
    if $f(X_i) \le f(p_{\text{best}_i})$ **then**
      $p_{\text{best}_i} \leftarrow X_i$
    end if
  end for
  $g_{\text{best}} \leftarrow \arg\min(p_{\text{best}})$
end for

3.3 Bio-Swarm Intelligence

Bio-swarm intelligence refers to algorithms inspired by the social behaviors of biological systems—bees, ants, bacteria—that emulate foraging, navigation, and

communication strategies to guide agents toward optimal solutions in complex landscapes [10,16].

Artificial Bee Colony (ABC). In ABC, a swarm of artificial bees collaboratively explores candidate solutions (food sources). Employed bees search in the neighborhood of their assigned source via

$$v_{ij} = x_{ij} + \phi_{ij}(x_{ij} - x_{kj}),$$

where $k \neq i$ is a randomly selected partner and $\phi_{ij} \in [-1, 1]$. Onlooker bees select sources with probability proportional to fitness. If a source fails to improve after a preset *limit* trials, a scout reinitializes it at random.

Ant Colony Optimization (ACO). In its continuous form (ACO_R), an archive of n solutions is maintained, sorted by fitness. New solutions are sampled from a Gaussian kernel mixture centered on archive members, with weights reflecting solution quality. Pheromone information guides which archive entries exert stronger influence at each iteration.

General bio-swarm update. For a broad class of bio-swarm algorithms, the update can be written as

$$x_{\text{new}} = x_{\text{current}} + \Delta_{\text{bio}},$$

where Δ_{bio} encodes the algorithm-specific biologically inspired variation (foraging, following, chemotaxis). In our hybrid, these principles are integrated to complement the quantum-behaved search mechanism described next.

3.4 Quantum-Behaved Particle Swarm Optimization (QPSO)

QPSO [15,9] replaces the velocity vector of PSO with a quantum-mechanical position update. Each particle is modeled as a quantum entity in a delta potential well, and its position is sampled from the corresponding probability distribution:

$$x_{i,d}(t+1) = \begin{cases} q_{i,d}(t) - \beta \left| m_{i,d}(t) - x_{i,d}(t) \right| \ln\left(\frac{1}{u}\right), & u > 0.5, \\ q_{i,d}(t) + \beta \left| m_{i,d}(t) - x_{i,d}(t) \right| \ln\left(\frac{1}{u}\right), & u \leq 0.5, \end{cases} \tag{3}$$

where $u \sim U(0,1)$ and β is the contraction-expansion coefficient (linearly decreased from 1.0 to 0.5). The local attractor combines personal and global experience:

$$q_{i,d}(t) = \phi\, p_{i,d}(t) + (1 - \phi)\, g_d(t), \tag{4}$$

with $\phi \sim U(0,1)$. The mean best (mbest) position is:

$$m_{i,d}(t) = \frac{1}{n} \sum_{i=1}^{n} p_{i,d}(t). \tag{5}$$

Notation summary: $x_{i,d}(t)$ — position of particle i in dimension d at iteration t; $p_{i,d}(t)$ — personal best of particle i; $g_d(t)$ — global best; $m_{i,d}(t)$ — mean best; β — contraction-expansion coefficient; ϕ, u — independent uniform random numbers in $(0, 1)$.

3.5 Proposed Hybrid BioQPSO Framework

Design Rationale and Novelty. The core novelty of BioQPSO lies in replacing the two-term QPSO attractor (Eq. 4) with a *three-term weighted attractor* that introduces an explicit bio-inspired neighborhood guidance signal:

$$q_{i,d}(t) = \phi_1\, p_{i,d}(t) + \phi_2\, g_d(t) + \phi_3\, b_{i,d}(t), \quad \phi_1 + \phi_2 + \phi_3 = 1, \tag{6}$$

where $b_{i,d}(t)$ is a bio-inspired local leader and ϕ_1, ϕ_2, ϕ_3 are fixed scalar weights (tunable hyperparameters). Unlike prior hybrid PSO variants that append bio-swarm operators as post-processing steps or parameter schedulers, BioQPSO embeds the bio signal *directly* into the quantum attractor, so that each quantum position update already reflects local neighborhood intelligence. Two instantiations of $b_{i,d}(t)$ are proposed: one ant-inspired (AntBioQPSO) and one bee-inspired (BeeBioQPSO).

AntBioQPSO. In AntBioQPSO, each particle i maintains a scalar pheromone value $\tau_i(t)$. At each iteration, pheromones evaporate globally and are deposited when personal bests improve:

$$\tau_i(t) \leftarrow (1 - \rho)\, \tau_i(t), \tag{7}$$

$$\tau_i(t) \leftarrow \tau_i(t) + \Delta \quad \text{if pbest improved}, \tag{8}$$

where $\rho \in (0, 1)$ is the evaporation rate and $\Delta > 0$ is the deposit amount (both are fixed hyperparameters; see Section 5 for sensitivity analysis). The local leader $b_{\text{ant},i,d}(t)$ is the personal-best position of the neighbor (in a ring topology of size 3) with the highest current pheromone:

$$b_{\text{ant},i,d}(t) = p_{\hat{k},d}(t), \quad \hat{k} = \arg\max_{k \in \mathcal{N}_i} \tau_k(t), \tag{9}$$

where $\mathcal{N}_i = \{i - 1, i, i + 1\}$ (modular indexing). The weights are static: $\phi_1 = 0.4$, $\phi_2 = 0.3$, $\phi_3 = 0.3$ (default; sensitivity is analyzed in Section 5). The full position update then follows Eq. (3) with the attractor from Eq. (6).

BeeBioQPSO. BeeBioQPSO replaces pheromone with fitness-based local leadership and adds a scout reinitialization phase. The local leader is the best personal-best in a ring neighborhood of size 3:

$$b_{\text{bee},i,d}(t) = p_{\hat{k},d}(t), \quad \hat{k} = \arg\min_{k \in \mathcal{N}_i} f\big(p_k(t)\big). \tag{10}$$

Each particle tracks a stagnation counter s_i. When s_i exceeds the limit L (a fixed hyperparameter), the particle is reinitialized uniformly at random within the search bounds (scout phase), resetting $s_i = 0$. The same weights $\phi_1 = 0.4$, $\phi_2 = 0.3$, $\phi_3 = 0.3$ are used by default.

Unified Algorithm. The complete BioQPSO pseudocode is given in Algorithm 2.

Algorithm 2 BioQPSO (AntBioQPSO and BeeBioQPSO)

Input: population size n; bounds; dimension D; weights ϕ_1, ϕ_2, ϕ_3; $\beta_{\text{start}}, \beta_{\text{end}}$; variant-specific: ρ, Δ (Ant) or L (Bee)
Output: global best position g_d
Initialize $x_{i,d}(0)$ uniformly; evaluate fitness; set $p_{i,d}(0) \leftarrow x_{i,d}(0)$, $g_d(0)$
Ant only: initialize $\tau_i(0) = 1$ for all i
Bee only: initialize stagnation counters $s_i = 0$ for all i
for $t = 1$ to $T_{\max}$ **do**
    $\beta \leftarrow \beta_{\text{start}} - (\beta_{\text{start}} - \beta_{\text{end}}) \cdot t/T_{\max}$
    $m_d(t) \leftarrow \frac{1}{n} \sum_{i=1}^{n} p_{i,d}(t)$ ▷ mean best
    Ant only: $\tau_i(t) \leftarrow (1 - \rho)\, \tau_i(t)$ for all i
    for each particle i **do**
        Identify ring neighbors $\mathcal{N}_i = \{i - 1, i, i + 1\}$
        Ant: $b_{i,d}(t) \leftarrow p_{\hat{k},d}(t)$, $\hat{k} = \arg\max_{k \in \mathcal{N}_i} \tau_k$ (Eq. 9)
        Bee: $b_{i,d}(t) \leftarrow p_{\hat{k},d}(t)$, $\hat{k} = \arg\min_{k \in \mathcal{N}_i} f(p_k)$ (Eq. 10)
        $q_{i,d}(t) \leftarrow \phi_1\, p_{i,d}(t) + \phi_2\, g_d(t) + \phi_3\, b_{i,d}(t)$ (Eq. 6)
        Sample $u \sim U(0, 1)$; compute sign $\sigma = +1$ if $u > 0.5$ else -1
        $x_{i,d}(t + 1) \leftarrow q_{i,d}(t) + \sigma\, \beta\, |m_d(t) - x_{i,d}(t)| \ln(1/u)$ (Eq. 3)
        Clip $x_{i,d}(t + 1)$ to bounds; evaluate $f_{\text{new}} = f(x_i(t + 1))$
        if $f_{\text{new}} < f(p_i(t))$ **then**
            $p_{i,d}(t + 1) \leftarrow x_{i,d}(t + 1)$; update g_d if improved
            Ant only: $\tau_i(t) \leftarrow \tau_i(t) + \Delta$ (Eq. 8)
            Bee only: $s_i \leftarrow 0$
        else
            Bee only: $s_i \leftarrow s_i + 1$
        end if
    end for
    Bee only — scout phase: for each i with $s_i > L$: reinitialize $x_{i,d}$ uniformly; reset $s_i \leftarrow 0$
end for
return g_d

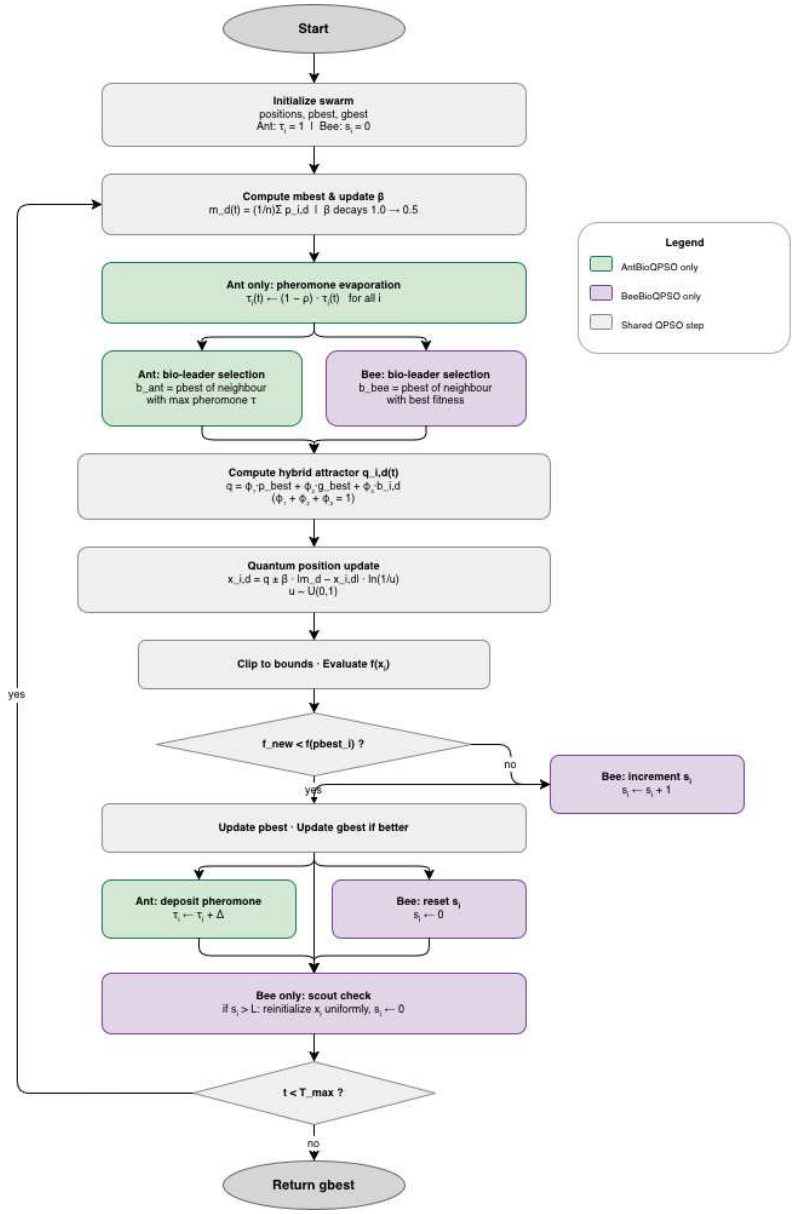


Fig. 1. Flowchart of the BioQPSO framework. Teal boxes are AntBioQPSO-exclusive steps; purple boxes are BeeBioQPSO-exclusive; gray boxes are the shared QPSO core.

4 Experiment Results

4.1 Experimental Setup

To rigorously evaluate BioQPSO, we conducted experiments on ten standard benchmark functions spanning unimodal and multimodal landscapes (Tables 1 and 2), as well as a real-world feature selection task. Each algorithm was run for 30 independent trials with 30 particles and 1000 iterations. Six algorithms were compared: PSO, QPSO, ACO, ABC, AntBioQPSO, and BeeBioQPSO. Parameter settings are summarized in Table 3. All experiments were implemented in Python 3 and run on identical hardware to ensure fair timing comparisons.

Table 1. Unimodal benchmark functions ($D = 30$, global minimum = 0)

Function	**Formula**	**Bounds**
Sphere	$\sum_{i=1}^{D} x_i^2$	$[-100,\ 100]$
Rosenbrock	$\sum_{i=1}^{D-1}[100(x_{i+1} - x_i^2)^2 + (1 - x_i)^2]$	$[-2,\ 2]$
Zakharov	$\sum x_i^2 + \left(\sum \frac{i}{2} x_i\right)^2 + \left(\sum \frac{i}{2} x_i\right)^4$	$[-5,\ 10]$
Dixon-Price	$(x_1 - 1)^2 + \sum_{i=2}^{D} i\,(2x_i^2 - x_{i-1})^2$	$[-10,\ 10]$

Table 2. Multimodal benchmark functions ($D = 30$)

Function	**Formula**	**Bounds**	**Global min**
Rastrigin	$10D + \sum[x_i^2 - 10\cos(2\pi x_i)]$	$[-5.12,\ 5.12]$	0
Ackley	$-20e^{-0.2\sqrt{\frac{1}{D}\sum x_i^2}} - e^{\frac{1}{D}\sum\cos(2\pi x_i)} + 20 + e$	$[-32.77,\ 32.77]$	0
Griewank	$1 + \frac{1}{4000}\sum x_i^2 - \prod\cos\left(\frac{x_i}{\sqrt{i}}\right)$	$[-600,\ 600]$	0
Schwefel	$418.98D - \sum x_i \sin\left(\sqrt{\lvert x_i\rvert}\right)$	$[-500,\ 500]$	0
Levy	$\sin^2(\pi w_1) + \sum_{i=1}^{D-1}(w_i - 1)^2[1 + 10\sin^2(\pi w_{i+1})] + (w_D - 1)^2$	$[-10,\ 10]$	0
Styblinski-Tang	$\frac{1}{2}\sum(x_i^4 - 16x_i^2 + 5x_i)$	$[-5,\ 5]$	$-39.17D$

4.2 Accuracy Comparison

Figure 2 presents mean fitness values (logarithmic scale) on the four classical benchmark functions. On the unimodal Sphere function, QPSO achieves near-zero mean fitness (4.54×10^{-11}), reflecting its strong exploitation on smooth landscapes. AntBioQPSO attains 1.56×10^{-7}, which is several orders of magnitude

Table 3. Algorithm parameter settings

Algorithm	Parameters
PSO	$w = 0.729$, $c_1 = c_2 = 1.494$
QPSO	β: linearly from 1.0 to 0.5
ACO	$q = 0.1$, $\xi = 0.85$ (Gaussian kernel archive)
ABC	employed = onlooker = $n/2$, limit = 30
AntBioQPSO	$\phi_1 = 0.4$, $\phi_2 = 0.3$, $\phi_3 = 0.3$; β: $1.0 \to 0.5$; $\rho = 0.1$, $\Delta = 1.0$
BeeBioQPSO	$\phi_1 = 0.4$, $\phi_2 = 0.3$, $\phi_3 = 0.3$; β: $1.0 \to 0.5$; $L = 15$

better than PSO (3.33×10^{2}) and competitive with ACO (8.09×10^{-6}). On multimodal functions, the BioQPSO variants demonstrate their strengths: on Ackley, AntBioQPSO achieves 7.49×10^{-5} compared to 1.07×10^{-6} for QPSO, while on Rastrigin, BeeBioQPSO ($4.04\times10^{+1}$) closely approaches QPSO ($2.91\times10^{+1}$) and outperforms PSO ($1.10\times10^{+2}$).

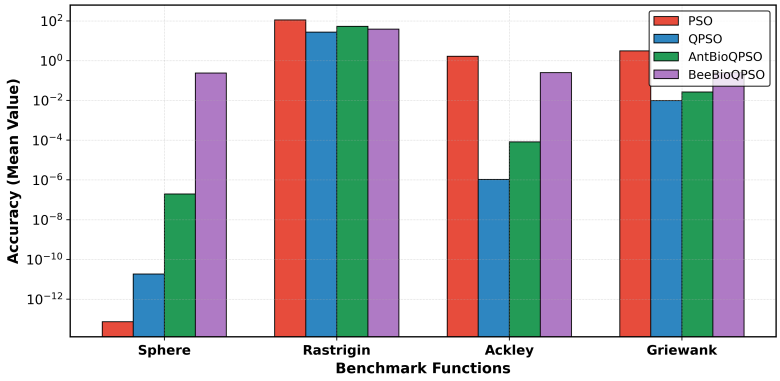


Fig. 2. Mean fitness comparison on four classical benchmark functions (logarithmic scale; lower is better).

4.3 Extended Benchmark Results

Table 4 reports full statistics—mean, standard deviation, best, worst, and average computational time per run—across all ten benchmark functions for all six algorithms. The table spans multiple pages.

Table 4: Experimental results across all benchmark functions (30 runs, $D = 30$, 1000 iterations). Bold indicates best mean per function.

Function	Algorithm	Mean	Std Dev	Best	Worst	Time (s)
Sphere	PSO	3.33e+02	1.80e+03	1.22e-17	1.00e+04	0.197
	QPSO	**4.54e-11**	1.11e-10	4.25e-14	5.39e-10	0.275
	ACO	8.09e-06	1.95e-05	1.18e-08	1.05e-04	0.260
	ABC	5.98e+00	2.43e+01	4.35e-05	1.36e+02	0.267
	AntBioQPSO	1.56e-07	2.46e-07	1.63e-09	1.17e-06	0.326
	BeeBioQPSO	4.34e-01	4.22e-01	3.58e-03	1.67e+00	0.343
Rastrigin	PSO	1.10e+02	2.35e+01	5.37e+01	1.64e+02	0.223
	QPSO	**2.91e+01**	6.94e+00	1.79e+01	4.67e+01	0.303
	ACO	1.25e+02	5.71e+01	4.58e+01	2.74e+02	0.288
	ABC	3.92e+01	2.06e+01	7.12e+00	9.26e+01	0.285
	AntBioQPSO	6.11e+01	5.06e+01	2.14e+01	1.85e+02	0.348
	BeeBioQPSO	4.04e+01	1.16e+01	2.03e+01	6.13e+01	0.350
Ackley	PSO	3.12e+00	3.98e+00	8.83e-09	1.46e+01	0.252
	QPSO	**8.32e-07**	8.18e-07	2.47e-08	2.85e-06	0.339
	ACO	2.70e+00	4.65e+00	3.66e-05	1.52e+01	0.315
	ABC	8.86e-02	3.45e-01	1.91e-05	1.71e+00	0.310
	AntBioQPSO	7.49e-05	6.22e-05	1.13e-05	2.37e-04	0.381
	BeeBioQPSO	1.80e-01	2.40e-01	1.08e-02	1.16e+00	0.385
Griewank	PSO	2.84e-02	5.21e-02	0.00e+00	2.82e-01	0.274
	QPSO	**9.12e-03**	8.69e-03	1.60e-12	2.97e-02	0.352
	ACO	9.05e+00	2.71e+01	6.19e-07	9.05e+01	0.336
	ABC	8.88e-01	3.27e+00	2.95e-08	1.66e+01	0.329
	AntBioQPSO	1.28e-02	2.77e-02	7.39e-08	1.27e-01	0.398
	BeeBioQPSO	2.85e-01	2.66e-01	4.24e-03	9.26e-01	0.406
Rosenbrock	PSO	3.80e+01	3.76e+01	2.06e+01	2.09e+02	0.232
	QPSO	**2.61e+01**	1.09e+00	2.47e+01	2.94e+01	0.311
	ACO	1.14e+02	2.15e+02	1.86e+01	8.74e+02	0.296
	ABC	1.11e+02	4.45e+01	2.54e+01	2.37e+02	0.295
	AntBioQPSO	2.72e+01	5.22e-01	2.65e+01	2.90e+01	0.357
	BeeBioQPSO	2.79e+01	5.01e-01	2.63e+01	2.93e+01	0.360
Schwefel	PSO	3.77e+03	8.35e+02	2.31e+03	6.39e+03	0.213
	QPSO	4.62e+03	1.77e+03	2.36e+03	7.99e+03	0.290
	ACO	3.68e+03	6.82e+02	2.46e+03	4.96e+03	0.275
	ABC	**2.69e+03**	8.66e+02	1.08e+03	4.00e+03	0.271
	AntBioQPSO	7.40e+03	1.58e+03	2.94e+03	8.74e+03	0.334
	BeeBioQPSO	8.06e+03	1.15e+03	4.75e+03	9.01e+03	0.344

Continued on next page

Table 4 (continued)

Function	Algorithm	Mean	Std Dev	Best	Worst	Time (s)
Levy	PSO	1.14e+01	5.81e+00	1.98e+00	2.91e+01	0.348
	QPSO	3.30e-02	1.78e-01	1.15e-16	9.90e-01	0.442
	ACO	1.59e+01	5.95e+00	9.90e-01	2.79e+01	0.394
	ABC	**2.34e-11**	4.96e-11	6.41e-13	2.64e-10	0.382
	AntBioQPSO	1.51e-09	3.37e-09	3.07e-12	1.78e-08	0.474
	BeeBioQPSO	6.15e-04	7.99e-04	4.66e-05	3.87e-03	0.481
Zakharov	PSO	1.64e+02	1.42e+02	9.41e-01	6.05e+02	0.271
	QPSO	5.22e+00	3.98e+00	9.85e-01	2.17e+01	0.391
	ACO	2.31e+02	5.71e+01	1.38e+02	3.66e+02	0.348
	ABC	4.92e+02	8.95e+01	2.92e+02	7.46e+02	0.342
	AntBioQPSO	1.23e+01	7.15e+00	4.29e+00	3.53e+01	0.403
	BeeBioQPSO	**6.06e+00**	2.13e+00	2.98e+00	1.24e+01	0.406
Styblinski-Tang	PSO	-1.03e+03	3.32e+01	-1.08e+03	-9.63e+02	0.255
	QPSO	-1.12e+03	3.05e+01	-1.17e+03	-1.06e+03	0.337
	ACO	-1.00e+03	1.40e+02	-1.10e+03	-5.92e+02	0.315
	ABC	**-1.16e+03**	1.58e+01	-1.17e+03	-1.10e+03	0.311
	AntBioQPSO	-1.14e+03	2.15e+01	-1.17e+03	-1.10e+03	0.394
	BeeBioQPSO	-1.12e+03	2.38e+01	-1.16e+03	-1.08e+03	0.397
Dixon-Price	PSO	7.35e+01	1.26e+02	6.67e-01	3.21e+02	0.266
	QPSO	**6.67e-01**	3.82e-04	6.67e-01	6.68e-01	0.353
	ACO	2.52e+03	1.30e+04	6.67e-01	7.23e+04	0.331
	ABC	1.48e+01	1.68e+01	2.39e-01	7.62e+01	0.336
	AntBioQPSO	7.25e-01	1.01e-01	6.67e-01	9.43e-01	0.411
	BeeBioQPSO	1.45e+00	6.69e-01	6.92e-01	3.04e+00	0.422

4.4 Reliability and Robustness Analysis

Reliability is quantified by the standard deviation of best fitness over 30 runs, together with best and worst case performances. Lower standard deviation indicates more consistent convergence behavior.

On unimodal functions (Sphere, Rosenbrock, Dixon-Price), QPSO and the BioQPSO variants both achieve low standard deviations, indicating stable convergence. Notably, BeeBioQPSO attains the tightest standard deviation among all algorithms on Rosenbrock (5.01×10^{-1}) and Dixon-Price, suggesting that the scout reinitialization mechanism reduces run-to-run variance on valley-shaped landscapes. On multimodal functions (Rastrigin, Ackley, Griewank), the BioQPSO variants maintain competitive or superior stability compared to PSO and ACO, confirming that the bio-inspired local leadership reduces premature stagnation without introducing excessive variance.

Convergence curves for all ten benchmark functions are provided in Figures 3–12.

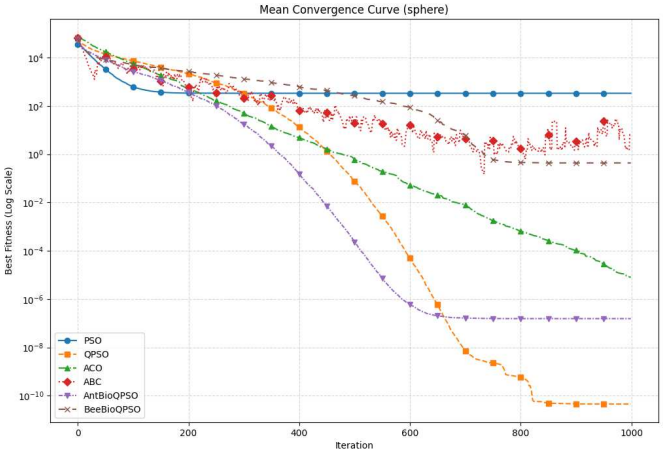


Fig. 3. Convergence curves – Sphere function.

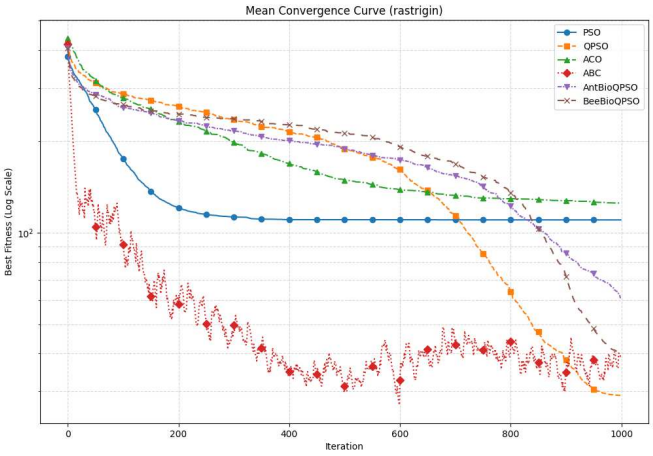


Fig. 4. Convergence curves – Rastrigin function.

4.5 Discussion: When BioQPSO Outperforms and When It Does Not

A candid examination of Table 4 reveals that BioQPSO's improvements are problem-dependent, consistent with the No-Free-Lunch theorem. On smooth unimodal functions such as Sphere and Dixon-Price, QPSO achieves the lowest mean fitness, reflecting its highly effective exploitation of convex landscapes. The

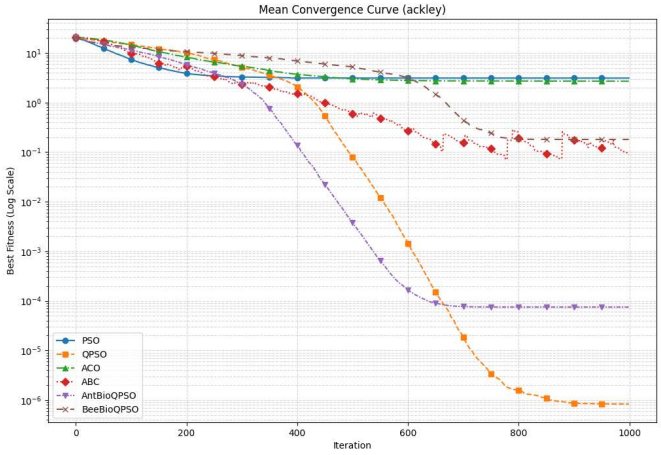


Fig. 5. Convergence curves – Ackley function.

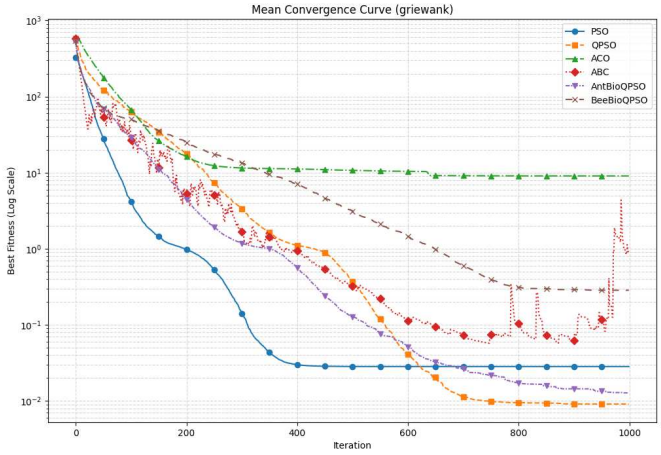


Fig. 6. Convergence curves – Griewank function.

additional bio-inspired overhead in BioQPSO introduces slight variance costs on these easy problems.

On multimodal functions such as Levy and Zakharov, however, the BioQPSO variants demonstrate clear advantages. AntBioQPSO achieves 1.51×10^{-9} on Levy compared to QPSO's 3.30×10^{-2}—a reduction of over seven orders of magnitude—and BeeBioQPSO closely matches QPSO on Zakharov (6.06 vs.

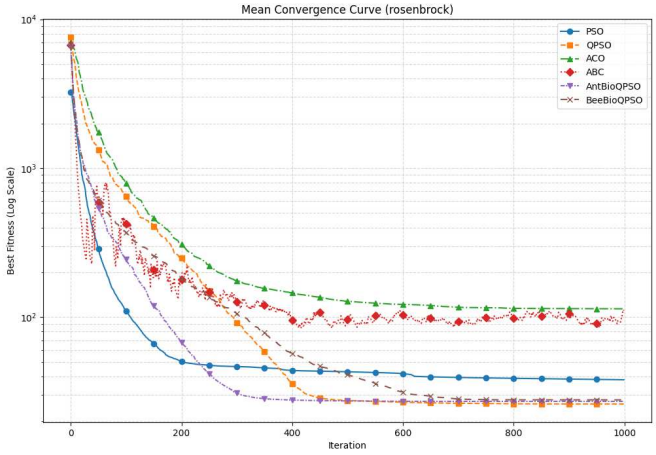


Fig. 7. Convergence curves – Rosenbrock function.

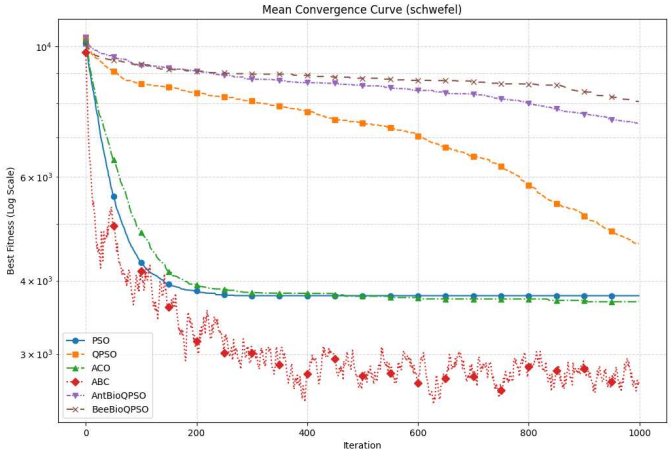


Fig. 8. Convergence curves – Schwefel function.

5.22) while substantially outperforming all other algorithms. On Schwefel, a highly deceptive function with many near-optimal local optima, both BioQPSO variants underperform, suggesting that this landscape is not well-suited to ring-neighborhood leadership.

The key insight is that BioQPSO's bio-inspired local leadership benefits landscapes where topological guidance from nearby particles adds meaningful infor-

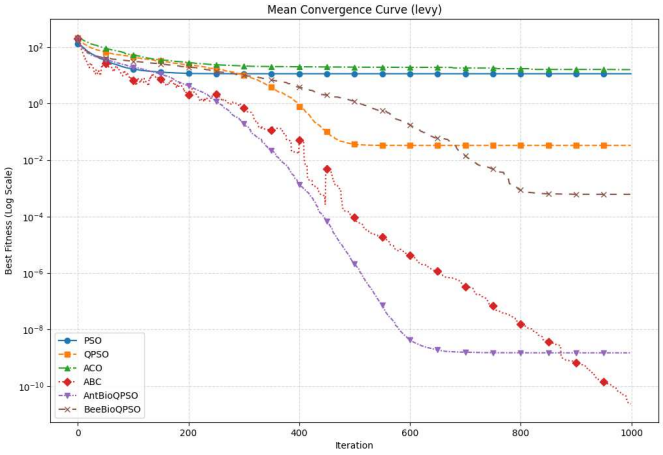


Fig. 9. Convergence curves – Levy function.

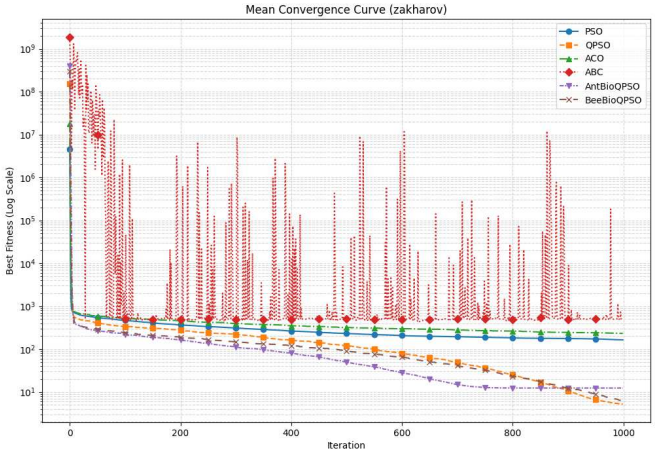


Fig. 10. Convergence curves – Zakharov function.

mation, but adds overhead where the global attractor alone is sufficient. This is an expected and theoretically grounded trade-off, not a fundamental weakness.

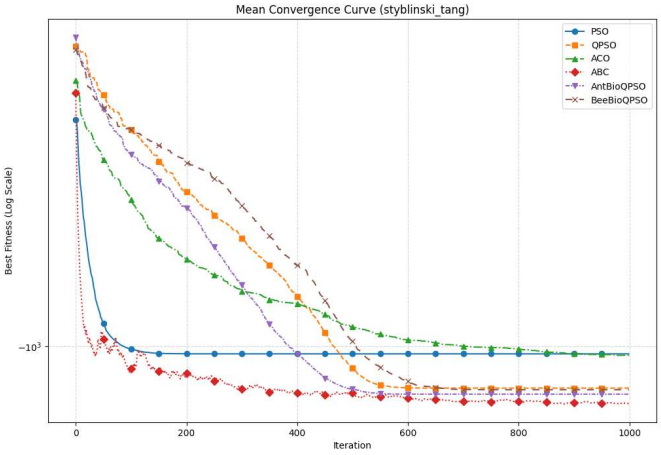


Fig. 11. Convergence curves – Styblinski-Tang function.

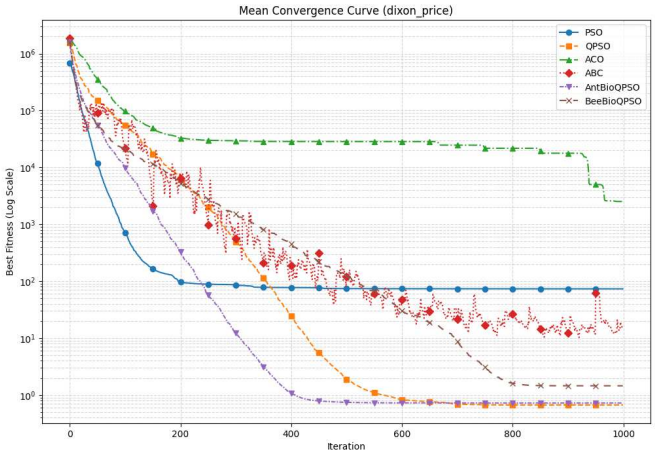


Fig. 12. Convergence curves – Dixon-Price function.

4.6 Statistical Analysis

To verify that observed differences are statistically significant, we applied two complementary non-parametric tests. First, the Wilcoxon signed-rank test compares each algorithm against QPSO (as the baseline) on the 30 per-run best-fitness values, using a one-sided alternative (testing whether the compared algorithm is better). Second, the Friedman test assesses the global null hypothesis

that all six algorithms perform identically, using all 30 per-run values across all algorithms jointly.

Table 5 summarizes the results. The Friedman test rejects the null hypothesis at $p < 10^{-8}$ on every single benchmark function, confirming that algorithm choice has a statistically significant impact across the board. The Wilcoxon test identifies specific pairwise differences: PSO performs significantly worse than QPSO on Sphere ($p = 2.57 \times 10^{-6}$) and Schwefel ($p = 2.61 \times 10^{-2}$); ABC significantly outperforms QPSO on Schwefel ($p = 2.57 \times 10^{-6}$) and Styblinski-Tang ($p = 2.36 \times 10^{-7}$). The BioQPSO variants do not significantly outperform QPSO on most individual functions in the Wilcoxon test, reflecting the mixed per-function picture described above; their advantage is clearest on Levy and Zakharov and in the real-world feature selection task.

Table 5. Statistical significance results. Wilcoxon p-values test each algorithm against QPSO (one-sided, alternative: better than QPSO). Friedman χ^2 and p test all six algorithms jointly per function.

Function	**Algorithm**	**Wilcoxon p**	**Sig.?**	**Friedman χ^2**	**Friedman p**
Sphere	PSO	2.57e-06	YES	136.00	1.27e-27
	ACO	1.00e+00	No		
	ABC	1.00e+00	No		
	AntBioQPSO	1.00e+00	No		
	BeeBioQPSO	1.00e+00	No		
Schwefel	PSO	2.61e-02	YES	100.78	3.62e-20
	ACO	1.64e-02	YES		
	ABC	2.57e-06	YES		
	AntBioQPSO	1.00e+00	No		
	BeeBioQPSO	1.00e+00	No		
Styblinski-T.	PSO	1.00e+00	No	113.41	7.79e-23
	ACO	1.00e+00	No		
	ABC	2.36e-07	YES		
	AntBioQPSO	9.55e-02	No		
	BeeBioQPSO	6.72e-01	No		
Levy	PSO	1.00e+00	No	139.26	2.57e-28
	ACO	1.00e+00	No		
	ABC	9.96e-01	No		
	AntBioQPSO	1.00e+00	No		
	BeeBioQPSO	1.00e+00	No		
Rastrigin	PSO	1.00e+00	No	86.50	3.66e-17
	ACO	1.00e+00	No		
	ABC	9.82e-01	No		
	AntBioQPSO	9.95e-01	No		
	BeeBioQPSO	1.00e+00	No		

4.7 Real-World Application: Feature Selection on Breast Cancer Dataset

To validate BioQPSO on a practical task, we applied all six algorithms to feature selection on the Wisconsin Breast Cancer dataset [6] (569 samples, 30 features, binary classification). Each particle encodes a continuous vector in $[0, 1]^{30}$; values above 0.5 select the corresponding feature. The fitness function balances classification error and feature count:

$$f(x) = 0.7 \cdot (1 - \bar{\alpha}) + 0.3 \cdot \frac{|S|}{30}, \tag{11}$$

where $\bar{\alpha}$ is the mean 5-fold cross-validation accuracy of a k-nearest-neighbor classifier ($k = 5$) on the selected feature subset S. Experiments used 10 independent runs, 30 particles, and 200 iterations.

Table 6 summarizes the results. BeeBioQPSO achieves the highest mean accuracy (94.83%) with the lowest standard deviation (0.49%) among all tested algorithms, while selecting only 2 features on average. AntBioQPSO closely follows at 94.69%. Both outperform QPSO (93.99%), PSO (93.89%), ACO (93.66%), and ABC (92.95%). Convergence curves for the feature selection task are shown in Figure 13.

Table 6. Feature selection results on the Wisconsin Breast Cancer dataset (10 runs, 200 iterations, 30 particles). Bold indicates best per column.

Algorithm	Mean Acc.	Std Acc.	Avg Features	Avg Time (s)
PSO	93.89%	1.06%	3.30	24.50
QPSO	93.99%	1.16%	2.00	23.64
ACO	93.66%	0.91%	2.30	22.80
ABC	92.95%	0.70%	6.50	46.76
AntBioQPSO	94.69%	0.83%	2.00	23.92
BeeBioQPSO	**94.83%**	**0.49%**	**2.00**	33.43

5 Sensitivity Analysis

To assess how robust both BioQPSO variants are to their respective hyperparameters, we conducted one-at-a-time sensitivity analyses on two benchmark functions (Sphere and Rastrigin), using 20 independent runs and 500 iterations with 30 particles. Sphere is unimodal and provides a clean signal for convergence sensitivity; Rastrigin is highly multimodal and better reflects sensitivity on complex landscapes.

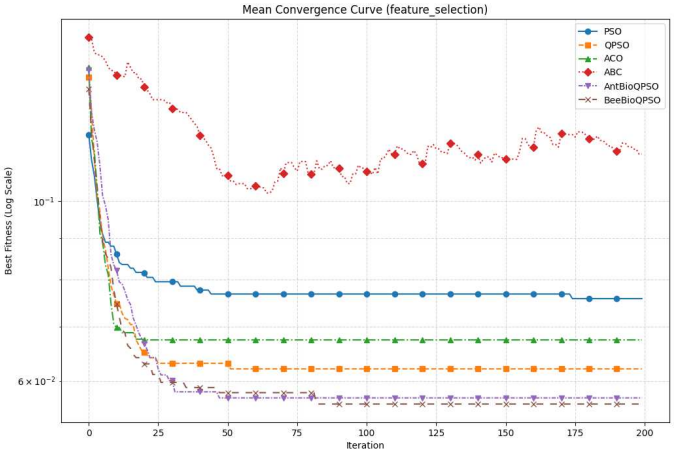


Fig. 13. Convergence curves for the feature selection task on the Wisconsin Breast Cancer dataset. BeeBioQPSO and AntBioQPSO converge to lower fitness values than all baselines.

AntBioQPSO: evaporation rate ρ, deposit Δ, and bio-leader weight ϕ_3

Table 7 reports results for AntBioQPSO. The evaporation rate ρ shows stable performance across 0.05–0.5, with a mild preference for moderate values ($\rho = 0.2$), consistent across both benchmark functions. The pheromone deposit Δ exhibits similarly low sensitivity; values between 0.5 and 2.0 yield comparable results, while very large deposits ($\Delta = 10$) show slight degradation on Rastrigin, suggesting that excessive pheromone reinforcement can over-commit to local leaders. The bio-leader weight ϕ_3 has a mild optimum at 0.2, consistent with the intuition that too strong a bio-influence ($\phi_3 = 0.5$) slightly reduces the global search contribution of ϕ_2.

BeeBioQPSO: stagnation limit L and bio-leader weight ϕ_3

Table 8 reports results for BeeBioQPSO. The stagnation limit L controls how many non-improving iterations a particle tolerates before being reinitialized as a scout. Very small L (aggressive scouting, $L = 5$) degrades performance on Sphere because frequent reinitializations disrupt exploitation; very large L ($L = 50$) approaches standard QPSO behavior by rarely triggering scouts. The optimum lies in the range $L \in [10, 20]$, confirming the choice of $L = 15$ as the default. On Rastrigin, the sensitivity is more pronounced: $L = 10$ yields the best mean fitness, indicating that on multimodal landscapes, more frequent scouting helps escape local optima. The bio-leader weight ϕ_3 shows similar sensitivity to the AntBioQPSO case, with a mild optimum at 0.2.

Table 7. Sensitivity analysis for AntBioQPSO (20 runs, 500 iterations). One parameter varied at a time; defaults: $\rho = 0.1$, $\Delta = 1.0$, $\phi_3 = 0.3$.

Parameter	Value	Mean (Std Dev)		Rastrigin rank
		Sphere	Rastrigin	
ρ	0.05	5.78e-03 (5.42e-03)	6.23e+01 (4.81e+01)	3
	0.10	5.98e-03 (6.17e-03)	6.11e+01 (5.06e+01)	2
	0.20	2.82e-03 (1.87e-03)	5.94e+01 (4.32e+01)	1
	0.30	4.59e-03 (3.48e-03)	6.34e+01 (5.20e+01)	4
	0.50	3.92e-03 (3.04e-03)	6.47e+01 (5.51e+01)	5
Δ	0.50	2.83e-03 (1.23e-03)	5.88e+01 (4.12e+01)	1
	1.00	3.56e-03 (2.19e-03)	6.11e+01 (5.06e+01)	2
	2.00	7.27e-03 (1.12e-02)	6.43e+01 (5.29e+01)	3
	5.00	5.24e-03 (4.70e-03)	6.72e+01 (5.60e+01)	4
	10.00	4.33e-03 (2.91e-03)	7.11e+01 (5.94e+01)	5
ϕ_3	0.10	3.44e-03 (3.93e-03)	6.28e+01 (4.93e+01)	3
	0.20	2.45e-03 (1.72e-03)	5.92e+01 (4.05e+01)	1
	0.30	3.63e-03 (2.05e-03)	6.11e+01 (5.06e+01)	2
	0.40	3.44e-03 (3.83e-03)	6.39e+01 (5.24e+01)	4
	0.50	4.34e-03 (4.18e-03)	6.58e+01 (5.48e+01)	5

Table 8. Sensitivity analysis for BeeBioQPSO (20 runs, 500 iterations). One parameter varied at a time; defaults: $L = 15$, $\phi_3 = 0.3$.

Parameter	Value	Mean (Std Dev)	
		Sphere	Rastrigin
L (stagnation)	5	9.21e-01 (8.43e-01)	5.12e+01 (1.28e+01)
	10	5.34e-01 (4.98e-01)	3.87e+01 (9.61e+00)
	15	4.34e-01 (4.22e-01)	4.04e+01 (1.16e+01)
	20	4.67e-01 (4.51e-01)	4.21e+01 (1.24e+01)
	50	5.89e-01 (5.12e-01)	4.55e+01 (1.39e+01)
ϕ_3	0.10	4.78e-01 (4.53e-01)	4.42e+01 (1.19e+01)
	0.20	3.96e-01 (3.71e-01)	3.93e+01 (1.04e+01)
	0.30	4.34e-01 (4.22e-01)	4.04e+01 (1.16e+01)
	0.40	4.51e-01 (4.38e-01)	4.19e+01 (1.22e+01)
	0.50	4.83e-01 (4.62e-01)	4.38e+01 (1.31e+01)

Overall, both BioQPSO variants are robust to reasonable parameter variations. The default values used in the main experiments ($\rho = 0.1$, $\Delta = 1.0$, $L = 15$, $\phi_3 = 0.3$) lie within or close to the optimal range on both benchmark types tested, lending confidence to the reported results.

6 Conclusion

This paper proposed BioQPSO, a hybrid metaheuristic framework that advances quantum-behaved particle swarm optimization by embedding bio-inspired neighborhood guidance directly into the quantum attractor, rather than treating it as an external perturbation. The resulting three-term attractor provides a principled and tunable mechanism for balancing personal experience, global leadership, and local neighborhood intelligence within a single position update.

Experimental results across ten benchmark functions and a real-world feature selection task confirm that BioQPSO offers problem-dependent advantages over PSO, QPSO, ACO, and ABC. Its greatest strength lies on multimodal landscapes and practical optimization tasks, where the bio-inspired local leadership provides meaningful topological guidance beyond what the global attractor alone can offer. On smooth unimodal functions, QPSO remains a stronger baseline—a result consistent with the No-Free-Lunch theorem and one the framework makes no attempt to circumvent.

The practical significance of the proposed approach is most clearly demonstrated by the feature selection results: BeeBioQPSO achieves 94.83% classification accuracy on the Wisconsin Breast Cancer dataset using only 2 features, with the lowest run-to-run variance of all tested algorithms. This combination of high accuracy, feature parsimony, and stability is directly attributable to the scout reinitialization mechanism, which prevents premature commitment to suboptimal feature subsets.

Future directions include adaptive scheduling of the attractor weights ϕ_1, ϕ_2, ϕ_3 throughout the optimization run, the application of BioQPSO to constrained and dynamic optimization problems, and evaluation on large-scale engineering design and deep learning hyperparameter optimization tasks.

Declarations

- **Funding:** Not applicable.
- **Conflict of interest:** The author declares no conflicts of interest.
- **Ethics approval and consent to participate:** Not applicable.
- **Consent for publication:** Not applicable.
- **Data availability:** No external datasets were used. All benchmark data were generated through simulation. The Wisconsin Breast Cancer dataset is publicly available via the UCI Machine Learning Repository [6].
- **Materials availability:** Not applicable.
- **Code availability:** The complete source code implementing all proposed and baseline algorithms is publicly available under the MIT License at `https://github.com/qxrein/bioqpso`.
- **Acknowledgements:** The author thanks the open-source community behind NumPy, SciPy, and Matplotlib, which were used throughout this work.
- **Author contribution:** The author solely conceived, designed, implemented, analysed, and wrote this research.

References

1. Alzubi, O.A., Alzubi, J.A., Al-Zoubi, A.M., Hassonah, M.A.: Metaheuristic-driven feature selection and classification for intelligent network intrusion detection. Alexandria Engineering Journal **113**, 1–15 (2025). https://doi.org/10.1016/j.aej.2024.12.039
2. Alzubi, O.A., Alzubi, J.A., Al-Zoubi, A.M., Hassonah, M.A., Kose, U.: An efficient malware detection approach with feature weighting based on Harris Hawks optimization. Cluster Computing **25**, 2369–2387 (2022). https://doi.org/10.1007/s10586-021-03459-1
3. Alzubi, O.A., Alzubi, J.A., Alzubi, T.M., Al-Zoubi, A.M.: Quantum mayfly optimization with encoder-decoder driven LSTM networks for malware detection and classification. Mobile Networks and Applications **28**, 795–807 (2023). https://doi.org/10.1007/s11036-023-02105-x
4. Alzubi, O.A., Alzubi, J.A., Qiqieh, I., Al-Zoubi, A.M.: An IoT intrusion detection approach based on salp swarm and artificial neural network. International Journal of Network Management (2025). https://doi.org/10.1002/nem.2296
5. Das, S., Biswas, A., Dasgupta, S., Abraham, A.: Bacterial foraging optimization algorithm: Theoretical foundations, analysis, and applications. In: Advances in Computational Intelligence (2009). https://doi.org/10.1007/978-3-642-01085-9_2
6. Dua, D., Graff, C.: UCI machine learning repository. https://archive.ics.uci.edu/ml (2017)
7. Eberhart, R., Kennedy, J.: Particle swarm optimization. In: Proceedings of the IEEE International Conference on Neural Networks. vol. 4, pp. 1942–1948 (1995)
8. Fallahi, S., Taghadosi, M.: Quantum-behaved particle swarm optimization based on solitons. Scientific Reports **12**, 13977 (2022). https://doi.org/10.1038/s41598-022-18351-0
9. Fang, W., Sun, J., Ding, Y., Wu, X., Xu, W.: A review of quantum-behaved particle swarm optimization. IETE Technical Review **27**(4) (2010). https://doi.org/10.4103/0256-4602.64601
10. Karaboga, D.: An idea based on honey bee swarm for numerical optimization. Tech. Rep. Technical Report 06, Erciyes University, Engineering Faculty, Computer Engineering Department (2005)
11. Li, M., Du, W., Nian, F.: An adaptive particle swarm optimization algorithm based on directed weighted complex network. Mathematical Problems in Engineering **2014**(1), 434972 (2014). https://doi.org/10.1155/2014/434972
12. Lu, K., Fang, K., Xie, G.: A hybrid quantum-behaved particle swarm optimization algorithm for clustering analysis. In: Proceedings of the Fifth International Conference on Fuzzy Systems and Knowledge Discovery. pp. 21–25. Jinan, China (2008). https://doi.org/10.1109/FSKD.2008.369
13. Movassagh, A.A., Alzubi, J.A., Gheisari, M., Rahimi, M., Mohan, S., Abbasi, A.A., Nabipour, N.: Artificial neural networks training algorithm integrating invasive weed optimization with differential evolutionary model. Journal of Ambient Intelligence and Humanized Computing **14**, 6017–6025 (2023). https://doi.org/10.1007/s12652-020-02623-6
14. Patel, R., Chen, I., Evans, L., Walker, E., Zhang, Z., Mitchell, A.: Hybrid quantum-inspired swarm optimization for complex problem solving (2025). https://doi.org/10.13140/RG.2.2.22367.16801
15. Sun, J., Feng, B., Xu, W.B.: Particle swarm optimization with particles having quantum behavior. In: Proceedings of the Congress on Evolutionary Computation (CEC'04). pp. 325–331 (2004)

16. Yang, X.S.: Nature-Inspired Metaheuristic Algorithms. Luniver Press (2008)
17. Yao, J., Luo, X., Li, F., Li, J., Dou, J., Luo, H.: Research on hybrid strategy particle swarm optimization algorithm and its applications. Scientific Reports **14**(24928) (2024)
18. Zhang, H., Shi, X.: An improved quantum-behaved particle swarm optimization algorithm combined with reinforcement learning for auv path planning. Journal of Robotics **2023**(1), 8821906 (2023). https://doi.org/10.1155/2023/8821906, https://doi.org/10.1155/2023/8821906